ELSEVIER

Carbohydrate Polymers 41 (2000) 207–217

Carbohydrate Polymers

www.elsevier.com/locate/carbpol

Shape, molecular weight distribution and viscosity of amylopectin in dilute solution

C.M. Durrani, A.M. Donald*

Cavendish Laboratory, Polymers and Colloids Group, Department of Physics, University of Cambridge, Madingley Road, Cambridge CB3 0HE, UK

Received 6 December 1994; received in revised form 30 January 1997; accepted 1 August 1997

Abstract

This paper presents results on the properties of amylopectin in solution using a variety of physical techniques. High-pressure liquid chromatography-multiple angle laser light scattering was used as a direct means to determine not only the number-average and weight-average molecular weights of a series of five amylopectin samples, but also their molecular weight distributions. Small angle X-ray scattering using synchrotron radiation revealed strong evidence to suggest that amylopectin is a manifestly non-spherical macromolecule in aqueous solution or dimethyl sulphoxide. Shear rate-dependent viscosity measurements showed that aqueous amylopectin solutions behave as Newtonian liquids up to a high concentration, with very little evidence for shear thinning at high shear rates. Viscosity data for different concentrations and two different molecular weights were successfully plotted in a reduced form to obtain a master plot, from which estimates for the polymer overlap concentration, c^*, were obtained.

Keywords: Molecular weight distributions; Shear rate-dependent viscosity; Polymer overlap concentration

1. Introduction

Amylopectin is a highly and non-randomly branched polysaccharide and is one of the two main components of starch, the other being the essentially linear molecule amylose. Amylopectin consists of D-glucopyranose monomers connected either through α-(1,4) or α(1,6) glycosidic bonds. Sequences of α-(1,4) connected monomers produce linear stretches of chain, whereas the α-(1,6) bonds act as branch points for further linear stretches.

Much of the work on amylopectin has concerned the elucidation of its complicated internal architecture, in terms of the number and arrangement of branches. Enzymatic debranching experiments (Robin, Mercier, Charbonniere & Guilbot, 1974) and experiments involving the enzymatic analysis of the products of acid degradation of amylopectin (Watanabe & French, 1980) provided evidence for two of the most plausible models: the French model and the Robin–Mercier model. Manners and Matheson supported a modified version of the French model (Manners & Matheson, 1981). Later, Burchard and Thurn (1985) used branching theory to build up molecular structures akin to the various proposed models of amylopectin and, on the basis of statistical calculations of the angular dependence of the light scattered from the different models, favoured a modified version of the Robin–Mercier model. The essential feature of these two similar models is that the amylopectin arranges itself into a tiered structure of "clusters".

Neither of the two models, however, provides any details of how amylopectin might behave in solution nor of the likely overall shape when solvated. Indeed, over the years, very little attention has been paid to this problem. This is particularly striking in comparison with the considerable interest which has been devoted to the behaviour of amylose in solution. It is, therefore, the purpose of this paper to contribute to the exploration of the physical properties of dilute solutions of amylopectin.

In its natural state, amylopectin has a very high molecular weight and can have a very broad distribution of molecular sizes, with polydispersities as high as 500 having been reported (Foster, 1965). It has, therefore, proved difficult to characterise fully the molecular weight distribution of amylopectin. Stacy and Foster (1956) summarised some of the early weight average molecular weight determinations using light scattering. All these fell in the range $10–420 \times 10^6$, depending on the source of the amylopectin. Banks, Geddes, Greenwood and Jones (1972) later obtained values ranging from 65 to 500×10^6. Some of these studies may however have over-estimated the molecular weight of amylopectin because of the weighting of light scattering in favour of a higher molecular weight material and, additionally, because of the tendency of even dilute solutions of

* Corresponding author.

0144-8617/00/$ - see front matter
PII: S0144-8617(99)00070-3

amylopectin to aggregate. On the other hand, techniques to measure number average molecular weight have the inherent defect that their sensitivity decreases with increasing molecular weight; the high molecular weight of amylopectin has, therefore, meant that osmotic pressure measurements, for example, are actually beyond their limits of sensitivity.

In this paper, we tackle the problem of amylopectin molecular weight determination using the relatively new technique of high pressure liquid chromatography multiple angle laser light scattering (HPLC-MALLS). This technique measures the light scattered at different angles from a polymer solution as it elutes from an HPLC column. A constant rate of flow enables the solution, separated according to molecular weight by the HPLC column, to be treated as a series of equally-sized volume 'slices', each of which takes a fixed length of time to flow through the scattering cell. The measurements on each slice allow the mass of each slice to be calculated, thereby allowing a direct determination of not only the weight average and number average molecular weight of the polymer, but also its molecular weight distribution.

Another matter of debate has concerned the shape of amylopectin in solution. Intuitively, one might expect this very bushy molecule to be spherical in solution, as is glycogen. Early on, however, Stacy and Foster (1957) believed that their light scattering measurements showed amylopectin not to be spherical, but 'more extended'. They proposed that it adopted a spherically symmetrical (yet unspecified) shape with a density distribution of matter which decreased continuously with distance from the centre. Later, Banks et al. (1972) claimed that the shape of amylopectin in dilute solution was related to the fact that amylopectin is synthesised in the amyloplast in a two-dimensional form (Banks & Greenwood, 1975). They suggested that although this planar structure collapses in on itself in dilute solution to give a spheroid, amylopectin is nevertheless capable of a considerable solvent expansion, reverting—in the asymptotic limit of infinite dilution—to its native two-dimensional form. It has been suggested (Callaghan & Lelievre, 1986) that the reason why amylopectin exists in a two-dimensional form in plants is because it enhances rigidity and limits swelling, enabling the plant to store a greater quantity of carbohydrate per unit volume of tissue than if amylopectin were three dimensional.

Recently, Callaghan and Lelievre (1985) provided experimental evidence for the significant planarity of wheat starch amylopectin in solution, through measurement of the self-diffusion coefficients of amylopectin and its solvent using pulsed-field gradient nuclear magnetic resonance. The solvent diffusion experiments showed that amylopectin could be described as an oblate ellipsoid in water, with an axial ratio of semi-major to semi-minor axes of eight. Additional evidence for the planarity of amylopectin was provided by analytical ultracentrifugation (Lelievre, Lewis & Marsden, 1986) and from theoretical modelling of the relationship between the concentration dependence of a polymer's self-diffusion coefficient and its macromolecular shape (Callaghan & Lelievre, 1986).

Despite the evidence which has been so far built up in the literature for amylopectin being a highly oblate ellipsoidal molecule in solution, there are, however, arguments in favour of an alternate picture, in which amylopectin behaves as a soft sphere, penetrable to solvent and of a non-uniform density. Simple branching theory, for example, would suggest a tree-like spherical structure because the branching, while certainly non-random locally, is approximately random over the whole molecule. Moreover, a soft sphere is only a time-averaged conformation, and even a linear coil appears highly asymmetric at a given instance (the average ratios of its mean-squared orthogonal x:y:z axes of 11.3:2.5:1 (Minato & Hatano, 1981) could by some criteria be interpreted as a disc).

In this paper, we use small angle X-ray scattering (SAXS) of synchrotron radiation to investigate the shape of amylopectin in water and dimethyl sulphoxide (DMSO) at a temperature at which aggregation is absent. In a SAXS experiment, the amplitude of radiation of wavelength λ, scattered at an angle θ, from a series of particles is the Fourier transform of the electron density distribution, $F(\mathbf{Q})$, over the volume V of each scattering particle

$$F(\mathbf{Q}) = \Delta\rho \int_0^\infty \cos(\mathbf{Q}\cdot\mathbf{r})\, \mathrm{d}V \tag{1}$$

where $Q = |\mathbf{Q}| = 4\pi \sin\theta/\lambda$, $\Delta\rho$ is the difference between the electron density of the particle (assumed to be constant) and that of the solvent, and $\mathbf{r}$ is the vector between each pair of electrons (Guinier, 1955). In the case of asymmetric particles, where the scattering is influenced by the average orientation of the particles relative to the incoming radiation, the intensity of the scattered radiation is the average of the square of $F(\mathbf{Q})$:

$$I(\mathbf{Q}) = \overline{F^2(\mathbf{Q})}. \tag{2}$$

The scattering from disc-like particles has been calculated on the basis of Eqs. (1) and (2) and is a well-known function (Kratky, 1982).

We first show that a simple model, which describes amylopectin as a hard sphere with a Gaussian distribution of sizes does not fit the SAXS data. Then, using the scattering formulae for thin discs, we show that our SAXS data suggest that amylopectin indeed is more disk-like. However, while acknowledging that our data do not disprove the arguments that amylopectin might behave as a soft sphere, we then go on to analyse our SAXS results on the assumption that amylopectin is disk-like, of uniform density and impenetrable to solvent. This simplistic approach allows us to make use of the scattering formula for thin discs, to compare our data with the theoretical scattering, and hence make an estimate for the size of the molecule.

Finally, we present results which investigate the dependence of the viscosity of amylopectin solutions on concentration and shear rate. We use these results to make an estimate for the polymer overlap concentration, c^* and to plot the viscosity data from samples of different molecular weight in reduced form on a master curve.

2. Experimental

2.1. Materials

The amylopectin samples used in this study were obtained from Unilever, and were prepared by pyrolysis of amylose-free waxy maize starch under dry acid conditions. Five samples labelled A, B, C, D and E were available, each of which had been pyrolysed for a different length of time. The samples were used without further treatment. When an aqueous slurry of the starch was viewed between the crossed polars of an optical microscope, granules with a typical 'Maltese cross' pattern were observed, indicating that the pyrolysis had retained the granules' crystalline structure. When the starch was heated to temperatures above ~70°C, however, the granules disintegrated to create an aqueous solution of amylopectin chains. After heating, no sign of the granular structure remained visible with the optical microscope. Solutions were made up in terms of the mass of polymer as a percentage of the total mass of polymer and solvent, by heating starch slurries to above 75°C.

2.2. High-pressure liquid chromatography multiple angle laser light scattering

Molecular weight measurements were made with a Wyatt Technology DAWN F (Wyatt, 1992). In this instrument, 18 detectors are arranged at different angles, θ, in a horizontal plane surrounding a cylindrical light scattering cell through which the polymer solution flows. Amylopectin solutions were made up to a concentration, c, of 2 mg ml^{-1} in an aqueous phosphate chloride buffer of strength 0.1 M and pH ~ 6.8 and were filtered through 0.45 μm millipore filters prior to measurement.

The excess Rayleigh ratio, R_θ, of the light scattered from the whole volume in the scattering cell was determined at each detector during the fixed time taken for each slice to flow through the cell. The concentration, c_i, of each slice was measured by a refractive index meter downstream from the light scattering cell, using a value for the specific refractive index increment, dn/dc, for amylopectin in water of 0.153 ml g^{-1} at a experimental wavelength of 632.8 nm (Greenwood & Hourston, 1975) which is approximately the same value as for amylopectin in the buffer solution. (Note that the value of c_i for each slice depends on the molecular weight of the polymer solution in the slice. The concentration of each successive slice is therefore different from the previous one, because the solution has been separated on the basis of molecular weight by the HPLC column.) These values for R_θ and c_i were then used to construct a Debye plot of (R_θ/K^*c) against $\sin^2(\theta/2)$ for each slice, where K^* is a constant (Marshall, 1978a). The mass of each slice, M_i, was determined from the value of the y-axis intercept, $(M_i - [2A_2cM_i^2])$, using a value for the second virial coefficient A_2 of 0.0 as measured at 25°C (Stacy & Foster, 1957; Banks et al., 1972; Huber, 1991). From each M_i, the number-average and weight-average molecular weights were then built up.

2.3. Ultracentrifugation

Sedimentation velocity studies were carried out on a Beckmann Model E analytical ultracentrifuge using Schlieren optics in single-sector centerpieces at a constant temperature of 21°C and with a top rotor speed of 59,780 rpm. A conventional sector-shaped cell did not allow the boundary to move away fast enough from the meniscus to make determination of sedimentation coefficients reliable. Instead, a synthetic boundary cell (Bowen & Rowe, 1970) was used which layered pure solvent onto the solution during centrifugation at which point a sharp, free boundary was immediately formed. Samples were made up to 0.5% (w/w) in an aqueous 0.15 M NaCl to minimise the effect of any ionic charges.

2.4. Small angle X-ray scattering

The scattering of X-rays from dilute solutions of amylopectin was obtained using synchrotron radiation of Station 8.2 at the Daresbury Laboratory. The X-ray beam is made monochromatic to a wavelength $\lambda = 0.154$ nm by a bent single crystal, and the high intensity of the beam means that the beam is made point-collimated. Detection of scattered X-rays was by a multi-wire position sensitive quadrant detector (Lewis, 1989).

Aqueous solutions of amylopectin of samples A, C and E were studied at different concentrations between 0.5 and 4% (w/w). Solutions of sample A were also made up in DMSO. Each solution was injected into the gap between two mica sheets glued onto a brass annular spacer of 0.5 mm thickness. The sample cell was placed in a sample holder which was held at a constant 65°C, to avoid the possibility of aggregation (Witnauer & Senti, 1955). For each sample, data were collected for 15 min. Measurements were made over several concentrations in order to observe the influence of interparticle interference on the scattering profile.

Raw data were divided by the response of the detector under uniform illumination to account for the differences in sensitivity at different positions on the detector. The resultant profiles were then normalised to account for variations in the beam intensity and for differences in sample thickness, by dividing by the integrated intensity of the beam measured by an ion chamber positioned after the sample. The background scattering was subtracted using normalised data from a cell filled with pure solvent. The relationship

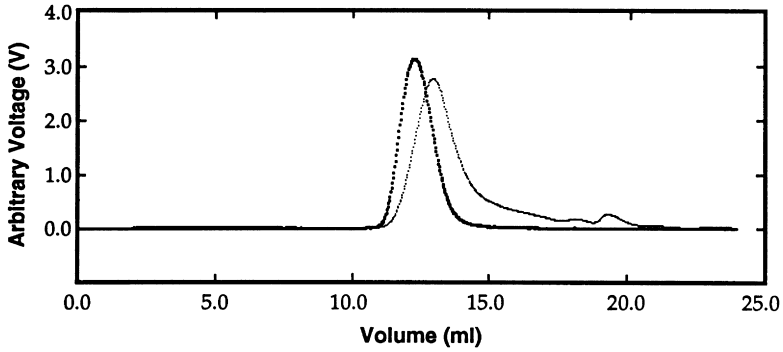

Fig. 1. The variation with elution volume of the light scattered from a 0.2% (w/v) solution of sample B measured by the detector at 90° to the direction of flow (—). Also shown is the variation with elution volume of the refractive index of the solution (—).

between detector channel number and Q value was established from the scattering of rat tail collagen.

2.5. Viscosity measurements

Viscosity measurements in this study were made at 25°C. Although amylopectin solutions of sufficient concentration can aggregate and (eventually) gel, this process is very slow even well below room temperature (Ring & Colonna, 1987). The temperature of 25°C was chosen to avoid the problem of solvent evaporation at higher temperatures, in the knowledge that over the time-scale of measurements, aggregation and gelation effects would, however, not be significant.

Intrinsic viscosity measurements were made with an Ubbelohde glass capillary viscometer immersed in a water bath maintained at a constant 24.99 ± 0.01°C, by measuring the relative viscosity $\eta_{rel} = \eta/\eta_s$ over a range of concentration, c, where η is the solution viscosity and η_s that of the pure solvent. The intrinsic viscosity, $[\eta]$, characterises the fractional increase in viscosity due to each solute molecule in isolation (Morris & Ross-Murphy, 1981), and is defined as the reduced viscosity $\eta_{red} = (\eta_{sp}/c)$ in the limit of infinite dilution,

$$[\eta] = \lim_{c \to 0} \left(\frac{\eta_{sp}}{c} \right) \tag{4}$$

where $\eta_{sp} = (\eta_{rel} - 1)$ is the specific viscosity of the solution. $[\eta]$ was calculated from the y-axis intercept of the straight-line fit to a 'Huggins' plot of η_{sp}/c against c and also from a 'Kraemer' plot of $\ln(\eta_{rel}/c)$ against c. The intrinsic viscosity for sample A was measured to be 0.177 ± 0.003 dl g^{-1} from the Huggins plot and 0.194 ± 0.008 dl g^{-1} from the Kraemer plot, and 0.107 ± 0.009 and 0.116 ± 0.005 dl g^{-1} for sample E.

Any liquid flowing through a capillary viscometer has a range of shear rates which increases radially from the centre of the tube. To ensure that the amylopectin solutions in the intrinsic viscosity measurements were within the Newtonian regime, the shear rate dependence of amylopectin solutions was measured with a Contraves Low Shear Viscometer and, for solutions well into the concentrated regime (above $\eta_{rel} >$ 50), with a Rheometrics RMS-605 Mechanical Spectrometer. Measurements were taken in the Couette geometry of the Contraves at 25°C at shear rates between 1 and 100 rad s^{-1} and with the Rheometrics at 25 ± 1°C in cone and plate configuration with a 5 cm radius cone and cone angle 0.1°, between 0.3 and 300 rad s^{-1}. Amylopectin solutions were found not to be significantly shear thinning at all, showing only a slight downturn in viscosity at shear rates above 100 rad s^{-1} for a 45% (w/w) solution of sample A and ∽ 60% (w/w) for sample E.

3. Results

3.1. High-pressure liquid chromatography multiple angle laser light scattering results

The light scattering and refractive index peaks of a typical amylopectin solution as it elutes from the HPLC column are shown in Fig. 1 for sample B. The light scattering peak was more symmetrical than the refractive index peak, which had a long tail and two small bumps at the low molecular weight end of the distribution. The light scattering does not pick up these features at the lower end of the distribution, presumably because it is less sensitive to lower molecular weight material.

Fig. 2 shows the relationship between the molecular weight of each volume slice and the volume of solvent, calculated for sample B from the raw data shown in Fig. 1. This elution plot shows the (expected) linear relationship between log M_i and volume, although there is some scattering in data points at the high and low ends of the distribution.

Fig. 3 shows the cumulative molecular weight distribution for sample B determined from Figs. 1 and 2, along with cumulative distributions for samples C and E. (Note that we have plotted the distributions in this way because the figure loses its clarity if the data are shown in the more conventional form of the number of molecules with mass M_i against M_i.) Although the amylopectin samples do have clearly distinguishable distributions, there is nevertheless a

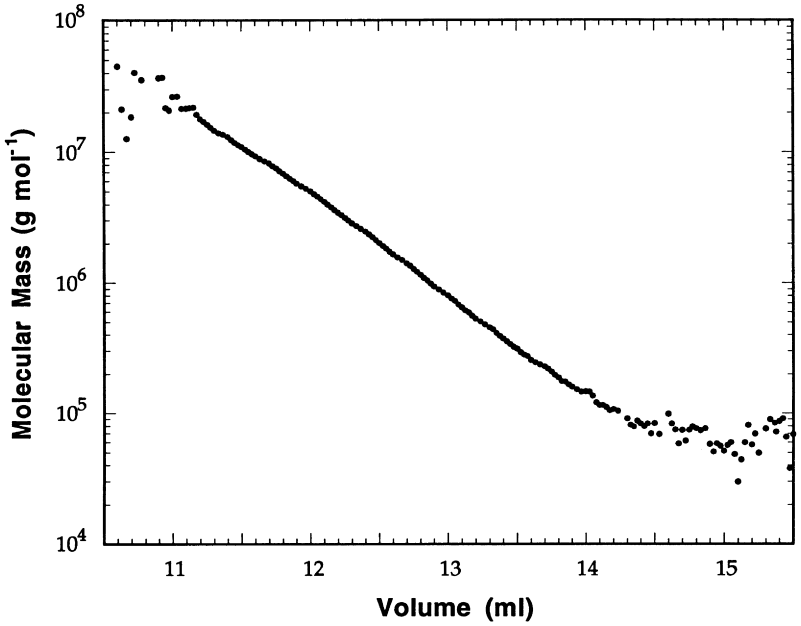

Fig. 2. The elution plot showing the variation of molecular weight with elution volume for the 0.2% (w/v) solution of sample B shown in Fig. 1.

considerable overlap between their distributions due to their high degree of polydispersity.

Experimental values of M_w and M_n for the five samples studied are given in Table 1. These values rank in increasing molecular weight, increasing with a decrease in the length of time for which the original waxy maize starch had been treated. Sample A, which had been treated with acid but not pyrolysed, was found to have a lower molecular weight than sample B. These weight-average molecular weights are two to three orders of magnitude less than measurements of the molecular weight of the undegraded amylopectin indicating the effect of the acid and heat treatment process to which the parent waxy maize starch was subjected.

The results gave polydispersity indices, M_w/M_n, which ranged between 3.6 and 8.3, indicating the wide range of molecular sizes present in each sample. These polydispersities are not as high as have been measured with other techniques. This may simply be because, our samples have lower molecular weights than the undegraded amylopectin samples used elsewhere, since a molecular weight

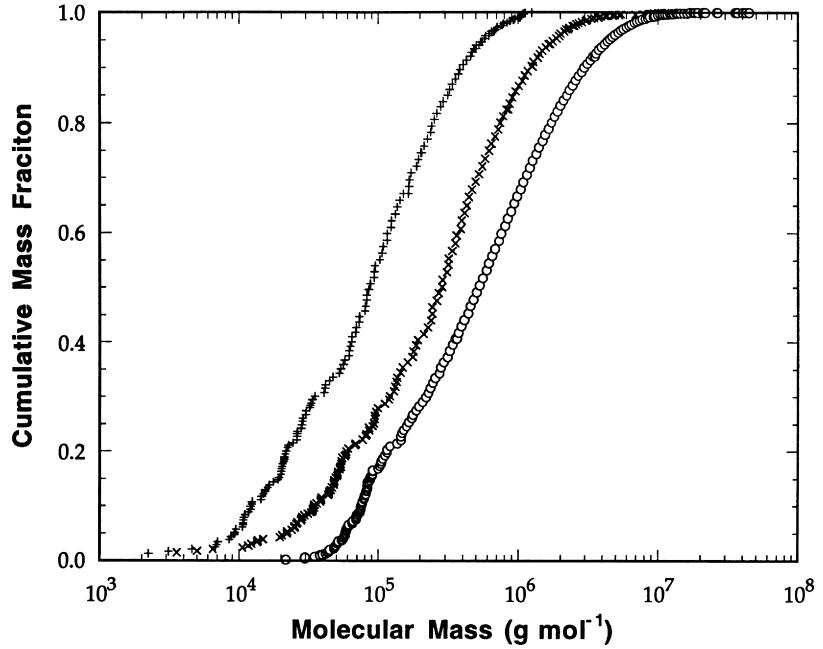

Fig. 3. The cumulative molecular weight distribution profiles for sample B (○) shown in Figs. 1 and 2, as well as ample C (×) and sample E (+).

Table 1
The weight-average and number-average molecular weights of the five amylopectin fractions measured by HPLC-MALLS. The errors are the standard deviations from at least four separate runs for each sample

Sample	M_n ($\times 10^{-5}$)	M_w ($\times 10^{-6}$)
Sample A	2.4 ± 0.5	1.07 ± 0.05
Sample B	2.0 ± 0.3	1.20 ± 0.04
Sample C	0.7 ± 0.1	0.58 ± 0.01
Sample D	0.7 ± 0.1	0.25 ± 0.01
Sample E	0.4 ± 0.01	0.20 ± 0.02

distribution moved to lower molecular weights will always reduce the polydispersity index. However, it may be that using a single technique to measure both M_n and M_w has produced more reliable values, and that other methods may have overestimated the polydispersity of amylopectin.

3.2. Sedimentation results

The ultracentrifugation of each of the amylopectin solutions produced a sedimentation peak which broadened significantly as it moved down the cell—indicating significantly polydispersity in sedimentation coefficient. The peak was also asymmetrically skewed to the side of a higher sedimentation coefficient.

In monodisperse solutions, the diffusion of polymers in the opposite direction to that in which the polymers are sedimenting causes the sedimentation peak to broaden symmetrically. Symmetrical broadening also occurs in systems with a symmetrical polydispersity in sedimentation coefficient. Hence the skewed broadening that we observed in the amylopectin solutions arose not only as a result of diffusion but also because of a skewing of the molecular weight distribution towards higher sedimentation coefficient (and hence high molecular weight). In the case of sample A, a small second peak was also observed, located on the high molecular weight 'tail', indicative of a bimodal distribution for that sample.

We did calculate values for the sedimentation coefficients of the peak of each distribution, but because of the high degree of polydispersity in the samples and the difficulty in locating the position of the peak, we do not believe our estimates were reliable and we have therefore not quoted them.

3.3. Small angle X-ray scattering results

The experimental scattering curves for solutions of sample E in water, after subtraction of solvent scattering, are shown in Fig. 4. The curves are all characterised by strong scattering at low Q which rapidly decreases at larger angles, with the amount of scattering increasing with increasing macromolecular concentration, as expected. However, when the scattering patterns were normalised, by dividing the scattered intensity by amylopectin concentration, a decrease in intensity with increasing concentration

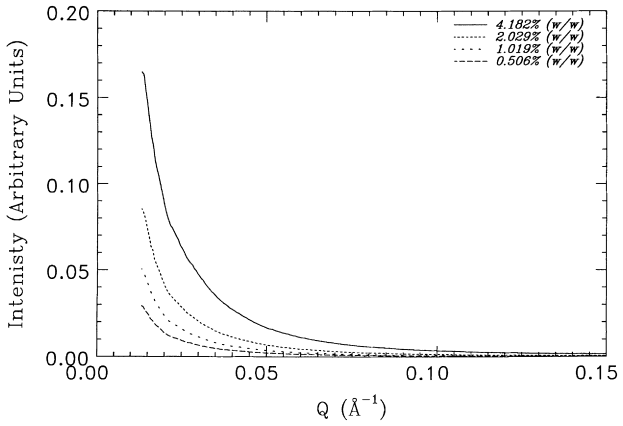

Fig. 4. Small angle X-ray scattering from aqueous solutions of amylopectin sample E in water after subtraction of solvent scattering. Four concentrations were studied: 0.50% (w/w) (– – –); 1.00% (w/w) (- - - -); 1.99% (w/w) (- - - -); and 4.01% (w/w) (—).

at low Q was observed. This indicated that even at these concentrations, there was some interparticle contribution to the scattering. A decrease in the normalised scattered intensity at low Q occurs because a correlation in position between different molecules reduces the structure factor at low Q to values below that of isolated macromolecules, whose structure factor is constant over all Q.

Attempts were conducted to fit the theoretical scattering from spheres of a uniform density, no solvent penetration and a Gaussian distribution of radii (to take into account the polydispersity) to the lowest concentration data in Fig. 4. This was done by first generating the theoretical SAXS profile from the spheres, by fixing either the central radius or the full width at half maximum of the distribution; and then trying to fit the SAXS profile to the data by allowing the other term, the relative intensity and the background to vary. However, none of these profiles managed to fit the data at all, despite using a number of different initial estimates for the central radii and the width of the distribution. This result indicates, at the very least, that such a model for amylopectin is inaccurate. Of course, this does not rule out that amylopectin might be spherical but with a variation in density across the molecule and/or with some degree of solvent penetration into the molecule.

However, plotting the experimental data from Fig. 4 in the form of ln(I) against ln(Q) for aqueous solutions of sample E revealed a striking linearity in the central region of the data (Fig. 5). Fig. 6 compares the data from solutions of sample A in water and DMSO, also revealing a strong linearity between ln(I) and ln(Q) although the scattering is slightly dependent on the solvent type. All the data had slopes which were close to -2 (Table 2), which in the limiting case of -2 indicates that the scattering arises from the presence of disc-shaped particles whose thickness is much less than the other two dimensions (Porod, 1982). The downturn in the slope at a high Q in Fig. 5 is because the intensity of any system of particles varies with Q^{-4} for high

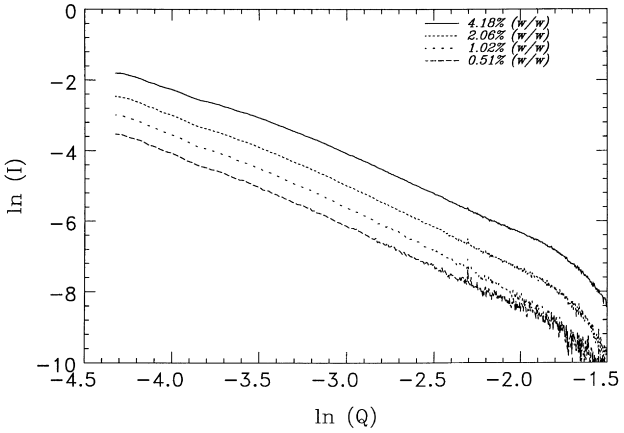

Fig. 5. Small angle X-ray scattering from solutions of amylopectin sample E in water after subtraction of solvent scattering plotted in the form ln(I) against ln(Q): 0.50% (– – –); 1.00% (- - - -); 1.99% (- - - -); and 4.01% (—).

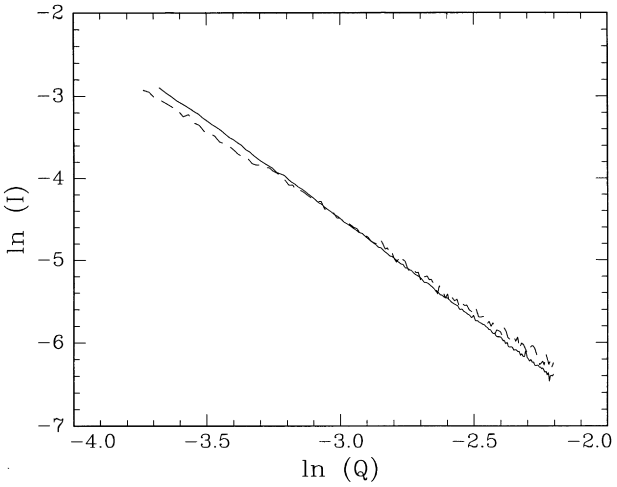

Fig. 6. SAXS data from solutions of amylopectin of sample E of comparable concentration in water and DMSO plotted in the form ln(I) against ln(Q): 3.02% (w/w) in H_2O (—) and 2.84% (w/w) in DMSO (- - - -).

Q, according to Porod's law. Figs. 5 and 6 are consistent, with the molecules being more disc-like than spherical.

The mathematical expression for the scattered intensity from a true thin disc is composed of two parts: the scattering due to the large cross-sectional shape, which is known to vary as Q^{-2}, and a thickness factor $I_t(Q)$ (Porod, 1982). Both factors can be treated separately when calculating $\overline{F^2(Q)}$ i.e. I(Q). When the variation of $I_t(Q)$ is modified using a Guinier-type approximation, I(Q) is then given by (Porod, 1982)

$$I(Q) = \frac{2\pi A}{Q^2}(\Delta\rho)^2 t^2 e^{-Q^2 R_t^2} \quad (5)$$

where A is the cross-sectional area of the disc. R_t is now the radius of gyration of the disc but refers only to the cross-section and is related to the thickness, t, according to

$$R_t = \frac{t}{\sqrt{12}}. \quad (6)$$

The expression for I(Q) in Eq. (5) holds in the central region of the scattering curve where $Qt < 1$ and $QR > 1$, where R is the radius of the disc, but breaks down outside these limits. The key point of Eq. (5) is that it indicates that disc-shaped particles have a linear relationship between ln (IQ^2) and (Q^2) in the central part of the data with a slope of $-R_t^2$. The data at low Q cannot be relied on in these analyses because as $Q \rightarrow 0$, the term IQ^2 must tend to zero. Furthermore, a lack of intensity at low Q is expected when the planar dimensions are only two or three times larger than the thickness, although even under these conditions determination of the thickness by evaluating the slope in the central part of the data is still valid (Pilz, 1982).

When the experimental data for aqueous solutions of sample E are plotted in this form of ln (IQ^2) against Q^2, the data are reasonably straight above $\backsim 0.03$ Å (Fig. 7). An indication of the thickness of the amylopectin molecules was thus obtained by assuming them to be true discs and measuring the slopes of the graphs in Fig. 7. Fig. 8 shows the least squares fit to the linear region of the data for the four solutions of sample E studied; the thicknesses obtained from the slopes using Eq. (6) are given in Table 3. Because the concentration dependence shows there to be an inter-particle scattering at the concentrations used, an extrapolation to infinite dilution is needed. This led to an estimate of 27 Å for the thickness of the isolated macromolecule of sample E (Fig. 9).

Table 3 also gives estimated thicknesses for sample A in water and DMSO, at the concentrations studied, again from linear fits to the data plotted in the form ln(IQ^2) against Q^2. An extrapolation to infinite dilution for sample A in water led to a thickness of 29.7 Å (Fig. 9). Thus, there is no

Table 2
The slopes of the SAXS data in the central portion of the data when plotted in the form ln(I) against ln(Q) for sample E amylopectin in aqueous solution and for sample A amylopectin in aqueous solution and in DMSO. Errors were obtained from the error in the fit to each data set

Sample E in H_2O		Sample A in H_2O		Sample A in DMSO	
Concentration % (w/w)	Slope	Concentration % (w/w)	Slope	Concentration % (w/w)	Slope
0.50	− 2.18 ± 0.01	0.51	− 2.598 ± 0.001		
1.00	− 2.22 ± 0.01	0.99	− 2.55 ± 0.01	1.73	− 2.23 ± 0.01
1.99	− 2.17 ± 0.01	3.02	− 2.42 ± 0.01	2.84	− 2.30 ± 0.01
4.01	− 2.03 ± 0.01				

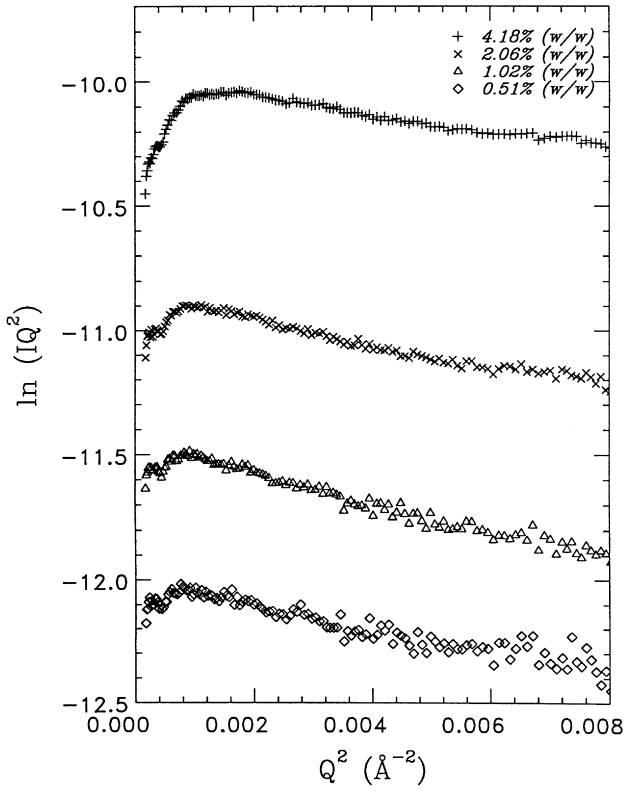

Fig. 7. SAXS data from solutions of amylopectin sample E in water, after subtraction of solvent scattering, plotted in the form $\ln(IQ^2)$ against Q^2: 0.5% (w/w) (◇); 1.02% (w/w) (△); 2.06% (w/w) (×); and 4.18% (w/w) (+).

significant difference in thickness between samples A and E, despite their very different molecular weights. Clearly, if amylopectin were indeed a thin disc, then these differences in molecular weight would be predominantly reflected by differences in the cross-sectional area.

The thickness of amylopectin macromolecules of sample A at 2.8% in DMSO, however, was found to be less, by about 10%, than in an aqueous solution at the comparable concentration of 3%, and less by about a third compared to the isolated macromolecule in water (Table 3). This suggests that amylopectin adopts an even more planar shape in DMSO than in water.

It must be stressed, however, that these values which we obtained only represent crude estimates of the size of amylopectin molecules, based on the assumption that the scattering formulae for thin discs can be applied to our data. Nevertheless, they do serve as a starting point for comparison with values obtained by other workers using different techniques.

3.4. Viscosity results

For polymer solutions, a double logarithmic plot of the viscosity extrapolated to zero shear rate against concentration shows a pronounced change in slope at a particular concentration, c^*. This concentration separates the dilute regime from the semi-dilute regime and marks the onset of polymer entanglement. c^* is inversely dependent on the hydrodynamic volume, which itself is related to the intrinsic viscosity. It has been shown that by plotting specific viscosity at zero shear against the coil-overlap parameter $c[\eta]$, viscosity–concentration data sets from different molecular weight fractions of the same polymer lie on a master curve (Morris, Cutler & Ross-Murphy, 1981).

The specific viscosity of amylopectin solutions of samples A and E showed very little shear rate dependence over the rates studied (Fig. 10). The absence of shear thinning indicates that the size of the molecules is such that their relaxation times are not long enough to show up as a function of shear rate. The specific viscosities were then

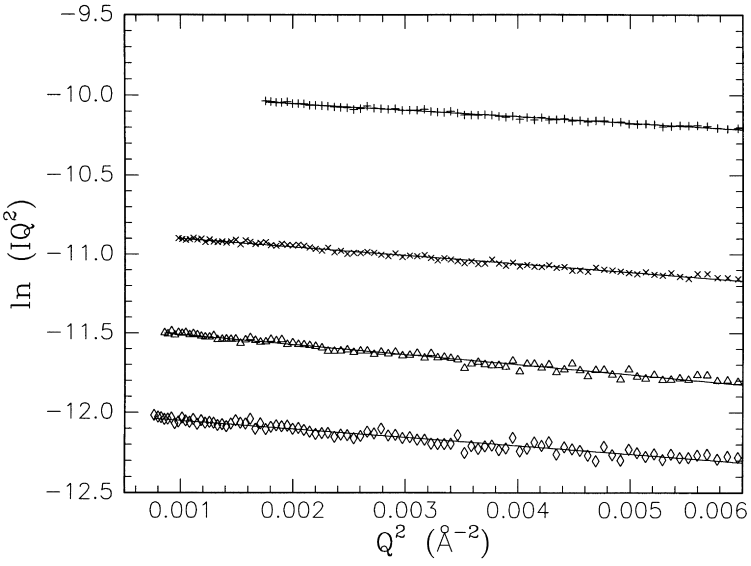

Fig. 8. Linear fits to the SAXS data from aqueous solutions of sample E plotted in the form $\ln(IQ^2)$ against Q^2: 0.50% (w/w) (◇); 1.00% (w/w) (△); 1.99% (w/w) (×) and 4.01% (w/w) (+).

Table 3
The thickness of amylopectin sample E in aqueous solution and of sample A amylopectin in aqueous solution and DMSO. Values were obtained by plotting the SAXS data in the form of Guinier thickness plots of $\ln(IQ^2)$ against Q^2, according to Eq. (5). Errors were obtained from the errors in the fit to each data set

Sample E		Sample A			
Concentration % (w/w)	Solvent: H_2O Thickness (Å)	Concentration % (w/w)	Solvent: H_2O Thickness (Å)	Concentration % (w/w)	Solvent: DMSO Thickness (Å)
0.50	25.2 ± 0.4	0.51	28.9 ± 0.6	1.73	21.9 ± 0.4
1.00	27.6 ± 0.3	0.99	27.6 ± 0.4	2.84	21.5 ± 0.5
1.99	25.4 ± 0.2	3.02	28.9 ± 0.3		
4.01	22.0 ± 0.2				

extrapolated to zero shear rate using a linear fit to the data at low frequency, and plotted on a master plot of $\log(\eta_{sp})$ against $\log(c[\eta])$ (Fig. 11). Agreement between the data from samples A and E was very good. This confirms the view (Ross-Murphy, 1984) that the concentration and shear rate dependence of the viscosity of polymer solutions can be rationalised by the molecular theories outlined above, with only the intrinsic viscosity acting as a normalising factor. This test has previously been applied to different molecular weight fractions of galactomannan, which behaves as a random coil (Robinson, Ross-Murphy & Morris, 1982), but is seen here to work as well for a highly branched system.

Two distinct regions can be seen in Fig. 11, each of which shows a linear dependence of η_{sp} on $c[\eta]$. At low $c[\eta]$, $\eta_{sp} \sim c^{1.1}$, followed by a curve of increasing gradient which became a straight line of $\eta_{sp} \backsim c^{4.4}$ at high $c[\eta]$. Although there was no discontinuity in the data characteristic of a sharp transition to the concentrated regime, this can be attributed to polydispersity of amylopectin, with different molecular weights showing different values of c^*. Nevertheless, a discontinuity can be estimated to occur at a value $c^*[\eta] \approx 2.4$, where the two linear regimes intersect. This value of $c^*[\eta]$ lies between the value of four obtained for most random coil polysaccharides, and 1.5 for spherical molecules (Ross-Murphy, 1984). However, it is not generally possible to infer molecular shapes from such viscosity data, and therefore, this value of $c^*[\eta]$ cannot be used to comment on the shape of amylopectin. From this value of $c^*[\eta]$, a c^* of 17.3% (w/w) is obtained for sample E and 11.6% (w/w) for sample A. These values for c^* are significantly higher than that of 0.9% (w/w) measured by Ring and co-workers on an undegraded amylopectin obtained from the waxy-maize starch (Ring & Colonna, 1987). Their surprisingly low value was quoted despite their correct assertion that, because of the presence of branching in amylopectin, the value for c^* ought to be higher than the value of 1.5% (w/w) they obtained for linear amylose of molecular weight 1.5×10^5. The values of c^* obtained here appear to be more reasonable in the light of their comments. The high values for c^* determined here indicate that because of the high degree of branching, far fewer inter-molecular entanglements show up for a given concentration than for amylose of the same molecular weight. The low value obtained by Ring may have been a consequence of having used only an Ubbelohde viscometer to measure viscosity; we found it imperative to use a Couette viscometer and a mechanical spectrometer to extend the range of concentrations fully into the concentrated regime.

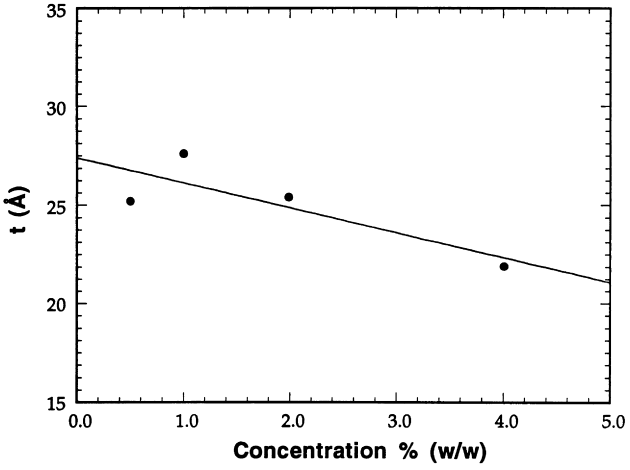

Fig. 9. Variation of the thickness of amylopectin of sample E with concentrations. Also shown is a linear fit to the data to obtain the extrapolated thickness at the limit of infinite dilution.

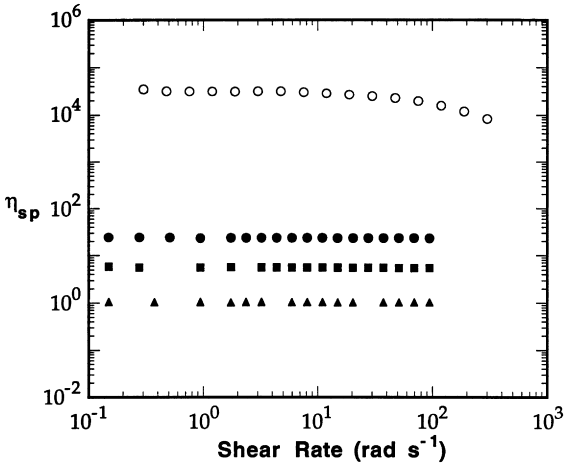

Fig. 10. Shear rate dependence of the specific viscosity, η_{sp}, of aqueous amylopectin solutions of sample E: 0.87% (w/w) (△); 10.7% (w/w) (□) 20.1% (w/w) (●) and 45.1% (w/w) (○).

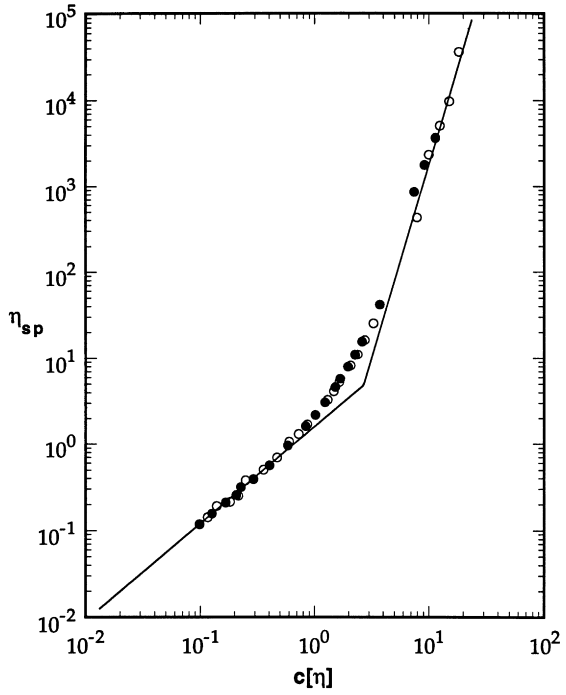

Fig. 11. Variation of zero shear specific viscosity with the coil overlap parameter $c[\eta]$ for the two amylopectin samples A (○) and E (●). Also shown are linear fits to the data at low $c[\eta]$ up to $c[\eta] = 0.12$ ($\eta_{sp} = 0.47$) and at high $c[\eta]$ beyond $c[\eta] = 0.69$ ($\eta_{sp} = 0.47$).

4. Discussion

4.1. Amylopectin polydispersity

The cumulative weight distribution profiles obtained from the HPLC-MALLS experiments ranked the five samples in a clear order with peaks in the distributions at different molecular weights. The profiles also show the high degree of polydispersity in the samples.

However, the polydispersity made it impossible to determine accurately the sedimentation coefficients of the amylopectin solutions in the ultracentrifugation experiments, because the sedimentation peak broadened so much as it moved down the cell. Clearly, when it comes to making quantitative estimates of amylopectin solutions, HPLC-MALLS is more effective than ultracentrifugation. However, ultracentrifugation of sample A did reveal an additional small peak in the sedimentation profile on the high molecular weight side of the distribution. This bimodality in the distribution for sample A was not revealed with the light scattering data, presumably because it is in some respects a less sensitive technique than ultracentrifugation.

4.2. Dimension of amylopectin in solution

We can compare our estimates for the thickness of amylopectin obtained from the SAXS data (made under the simplistic assumption that it behaves as a solvent-impenetrable true thin disc of a uniform density) with the values obtained in the studies by Lelievre and co-workers for the semi-major axis, *a*, and the semi-minor axis, *b*, of amylopectin as an oblate ellipsoid.

These workers, however, found a significant difference in the axial dimensions of amylopectin depending on whether the solvent was water or DMSO. This difference was attributed by them to the aggregation of amylopectin macromolecules in water, but not in DMSO. For example, by measuring the value of the amylopectin self-diffusion coefficient at an infinite dilution using NMR, Callaghan and Lelievre (1985) obtained estimates for the size of amylopectin from wheat starch cv. Gamenya of $a = 1200$ and $b = 150$ Å in water and $a = 220$ and $b = 12$ Å in DMSO. However, we minimised the effects of aggregation in our SAXS experiments, not only by using samples with a considerably smaller molecular weight than those used by Lelievre (Callaghan & Lelievre, 1985; 1986), but also by working at concentrations well below c^* and at an elevated temperature of 65°C. Therefore, to make valid comparisons between the dimensions deduced by Lelievre et al. and our results, only the data in DMSO, in which aggregation effects in their samples can be discounted, should be considered.

One simple comparison can be made by comparing the value of $2b$ obtained by Lelievre in DMSO with the value of the disk thickness, *t*, obtained here in DMSO. In this respect, the thickness of $\backsim 22$ Å for sample A in DMSO compares favourably with that of $2b = 24$ Å for amylopectin from wheat starch cv. Gamenya (Callaghan & Lelievre, 1985) and wheat starch cv. Crossbow measured using analytical ultracentrifugation (Lelievre et al., 1986), but is approximately three times less than that of $2b = 86$ Å measured by these workers on amylopectin from wheat starch cv. Aotea using a model, which related the concentration dependence of the polymer self-diffusion coefficient to its macromolecular shape (Callaghan & Lelievre, 1986). We can, however, conclude that the SAXS data produces molecular dimensions of the same order of magnitude as obtained in the earlier studies of Lelievre.

Since, aggregation was absent in our samples for the reasons outlined above, the observed reduction in the nominal thickness of the molecule in DMSO compared to water (Table 3), indicates that DMSO does indeed affect the shape of amylopectin.

It is, of course, more valid not to assume that amylopectin is a disc of constant thickness, but to describe the molecule as an oblate ellipsoid of a certain axial ratio, and attempt to work out this ratio. One simple method to do this involves using sedimentation coefficient data, as these are related not only to the molecular weight of the macromolecules, but also to their frictional coefficients, which in turn are dependent on particle shape and the nature of the solvent (Marshall, 1978b). However, we were unable to accurately determine the sedimentation coefficients of the peak of each distribution, and so were unable to get reliable results from this approach.

5. Conclusion

This paper reports results on the properties of amylopectin in dilute solution using a number of physical techniques. HPLC-MALLS proved to be an effective method to establish the molecular weight distributions of amylopectin despite the fact that ultracentrifugation qualitatively indicated these distributions to be very broad. HPLC-MALLS was also able to distinguish between the five samples used in this study and provide values for their weight average and number average molecular weights. As a result of the manner in which the parent starch was treated, the molecular weights were found to be significantly less than those measured in the literature for undegraded amylopectin samples. All the samples also showed considerable polydispersity which ranged between 3.6 and 8.3.

Viscosity measurements showed that amylopectin solutions were not significantly shear-thinning. Viscosity data for different concentrations and two different molecular weights were successfully plotted in reduced form to obtain a master plot of η_{sp} against $c[\eta]$, from which values for c^* were obtained.

This work is also believed to report the first SAXS study of amylopectin solutions. Based on existing evidence for the highly oblate ellipsoidal shape of amylopectin by Lelievre and co-workers (Callaghan & Lelievre, 1985; 1986; Lelievre et al., 1986), an estimate for the size of the amylopectin molecules was made by assuming them to be solvent-impenetrable disks of an uniform density and plotting the SAXS data in the form $\ln(IQ^2)$ against Q^2. The radius of gyration of thickness at infinite dilution was estimated from these plots to be 27 Å for sample E and 29 Å for sample A. The effect of DMSO as a solvent was found to change the scattering from that in an aqueous solution, and produce a reduction in the nominal thickness of the macromolecule when the data were plotted as $\ln(IQ^2)$ against Q^2.

Acknowledgements

The authors would like to thank the Agricultural and Food Research Council and Unilever Research for funding this work and for providing a Ph.D. studentship to M. Durrani. We thank W. Bras, the station scientist on Station 8.2 at the Daresbury Laboratory, as well as Drs R.E. Cameron and P. Jenkins for help with the SAXS experiments; we also thank Drs S. Harding and J. Horton at the University of Nottingham for allowing use of the light scattering apparatus. N. Buttress performed the ultracentrifugation experiments. Finally we thank Drs A. Clark, P. Johnson and Professor S.B. Ross-Murphy for useful discussions.

References

Banks, W., Geddes, R., Greenwood, C. T., & Jones, I. G. (1972). *Stärke*, *24* (8), 245–250.

Banks, W., & Greenwood, C. T. (1975). *Starch and its components*, (pp. 30–51). Edinburgh: Edinburgh University Press.

Bowen, T. J., & Rowe, A. J. (1970). *An introduction to ultracentrifugation*, pp. 15–30. London: Wiley Interscience.

Burchard, W., & Thurn, A. (1985). *Macromolecules*, *18*, 2072–2082.

Callaghan, P. T., & Lelievre, J. (1985). *Biopolymers*, *24*, 441–460.

Callaghan, P. T., & Lelievre, J. (1986). *Analytica Chimica Acta*, *189*, 145–166.

Foster, J. F. (1965). Physical properties of amylose and amylopectin in solution. In R. L. Whistler & E. F. Paschall (Eds.), *Starch: chemistry and technology*, (p. 349). New York: Academic Press.

Greenwood, C. T., & Hourston, D. J. (1975). *Polymer*, *16*, 474–476.

Guinier, A. (1955). *Small angle scattering of X-rays*, pp. 5–82. New York: Chapman and Hall.

Huber, A. (1991). *Biochemistry Society Transactions*, *19*, 505–506.

Kratky, O. (1982). A survey. In O. Glatter & O. Kratky (Eds.), *Small angle X-ray scattering*, (p. 1). London: Academic Press.

Lelievre, J., Lewis, J. A., & Marsden, K. (1986). *Carbohydrate Research*, *153*, 195–203.

Lewis, R. (1989). Daresbury Delay Line Detectors and Data Acquisition Systems. Daresbury Laboratory, UK.

Manners, D. J., & Matheson, N. K. (1981). *Carbohydrate Research*, *90*, 99–110.

Marshall, A. G. (1978a). *Biophysical chemistry: principles, techniques and applications*, (pp. 479–480). New York: Wiley.

Marshall, A. G. (1978b). *Biophysical chemistry: principles, techniques and applications*, (pp. 197–200). New York: Wiley.

Minato, T., & Hatano, A. (1981). *Macromolecules*, *14*, 1035–1038.

Morris, E. R., Cutler, A. N., Ross-Murphy, S. B., & Rees, D. A. (1981). *Carbohydrate Polymer*, *1*, 5–21.

Morris, E. R., & Ross-Murphy, S. B. (1981). *Techniques in Carbohydrate Metabolism*, *B310*, 1–46.

Pilz, I. (1982). Proteins. In O. Glatter & O. Kratky (Eds.), *Small angle X-ray scattering*, (p. 239). London: Academic Press.

Porod, G. (1982). General theory. In O. Glatter & O. Kratky (Eds.), *Small angle X-ray scattering*, (p. 17). London: Academic Press.

Ring, S. G., Colonna, P. C., I'Anson, K. J., Kalichevsky, M. T., Miles, M. J., Morris, V. J., & Orford, P. D. (1987). *Carbohydrate Research*, *162*, 277–293.

Robin, J. P., Mercier, C., Charbonniere, R., & Guilbot, A. (1974). *Cereal Chemistry*, *51*, 389–405.

Robinson, G., Ross-Murphy, S. B., & Morris, E. R. (1982). *Carbohydrate Research*, *107*, 17–32.

Ross-Murphy, S. B. (1984). Rheological methods. In H. W. Chan (Ed.), *Biophysical methods in food research*, (p. 138). Oxford: Blackwell Scientific.

Stacy, C. J., & Foster, J. F. (1956). *Journal of Polymer Science*, *20*, 57–66.

.015w>Stacy, C. J., & Foster, J. F. (1957). *Journal of Polymer Science*, *25*, 39–50.

Watanabe, T., & French, D. (1980). *Carbohydrate Research*, *84*, 115–123.

Witnauer, L. P., Senti, F. R., & Stern, M. D. (1955). *Journal of Polymer Science*, *16*, 1–17.

Wyatt, P. (1992). Combined differential light scattering with various liquid chromatography separation techniques. In S. E. Harding & D. B. Sattelle & V. A. Bloomfield (Eds.), *Laser light scattering in biochemistry*, (p. 35). Cambridge: Royal Society of Chemistry.